



Published in final edited form as:

*J Immunol.* 2015 November 15; 195(10): 4913–4921. doi:10.4049/jimmunol.1500953.

## SARM1, not MyD88, mediates TLR7/TLR9-induced apoptosis in neurons<sup>1</sup>

Piyali Mukherjee<sup>\*,‡,2</sup>, Clayton W. Winkler<sup>\*,2</sup>, Katherine G. Taylor<sup>\*,2</sup>, Tyson A. Woods<sup>\*</sup>, Vinod Nair<sup>†</sup>, Burhan A. Khan, and Karin E. Peterson<sup>\*,3</sup>

<sup>\*</sup>Laboratory of Persistent Viral Diseases, Rocky Mountain Laboratories (RML), National Institute of Allergy and Infectious Diseases (NIAID), National Institutes of Health (NIH), Hamilton, MT 59840

<sup>†</sup>Research Technologies Branch, Microscopy Unit, RML, NIAID, NIH, Hamilton, Montana, USA

### Abstract

Neuronal apoptosis is a key aspect of many different neurological diseases, but the mechanisms remain unresolved. Recent studies have suggested a mechanism of innate immune-induced neuronal apoptosis that may act through the stimulation of toll-like receptors (TLR) in neurons. TLRs are stimulated both by pathogen associated molecular patterns (PAMPs) as well as by damage-associated molecular patterns (DAMPs), including micro-RNAs released by damaged neurons. In the current study, we identified the mechanism responsible for TLR7/TLR9-mediated neuronal apoptosis. TLR-induced apoptosis required endosomal localization of TLRs but was independent of MyD88 signaling. Instead, apoptosis required the TLR adaptor molecule, sterile alpha armadillo motif (SARM1), which localized to the mitochondria following TLR activation and was associated with mitochondrial accumulation in neurites. Deficiency in SARM1 inhibited both mitochondrial accumulation in neurites and TLR-induced apoptosis. These studies identify a non-MyD88 pathway of TLR7/TLR9 signaling in neurons and provide a mechanism for how innate immune responses in the CNS directly induce neuronal damage.

### INTRODUCTION

Neuronal damage or loss is a key pathological feature of multiple neurodegenerative disorders of both known and unknown etiologies. Understanding the underlying mechanisms of neuronal damage or apoptosis is important in developing potential therapeutic treatments for neurological diseases. However, the events that lead to neuronal apoptosis are often unclear, particularly in cases where neuronal death is not associated with a direct infection of the neuron by a pathogen. In these cases, neuronal cell death may occur via the activation of other mechanisms including innate immune responses.

<sup>1</sup>This research was supported by the Intramural Research Program of the National Institute of Allergy and Infectious Diseases.

<sup>3</sup>corresponding author: Rocky Mountain Laboratories, NIAID, 903 S. 4<sup>th</sup> St., Hamilton, MT, 59840. petersonka@niaid.nih.gov, phone: 406-375-9630. Fax: 406-363-9286.

<sup>4</sup>current address: Department of Biological Sciences, Presidency University, 86/1 College Street, Kolkata-700073, West Bengal, India.

<sup>2</sup>authors contributed equally to this work

One possible source of innate immune activation during both pathogen and non-pathogen related damage in the CNS is the production of damage associated molecular patterns (DAMPs). Damaged cells in the CNS may release exosomes containing microRNA and/or fragmented cellular DNA from dying cells, which can stimulate endosomal toll like receptors (TLRs) (1–4). Unlike glia or infiltrating immune cells, where TLR stimulation induces cytokine production and/or proliferation, TLR stimulation of neurons appears to have negative effects on neuronal morphology and physiology, often leading to neuronal degeneration (1, 5–8). In particular, stimulation of endosomally located TLRs (TLR3, TLR7, TLR8 and TLR9) expressed by neurons induces neuronal cell death (1, 5, 6, 8), however the mechanisms underlying this process remain unresolved. Although some studies have indicated a MyD88 dependent mechanism of cell death (1, 2), others have indicated a MyD88-independent mechanism (8, 9) suggesting that novel TLR signaling pathways may contribute to neuronal damage.

Each of the twelve known TLRs bind to members of the highly conserved TIR-containing adaptor protein family which in turn initiate signal transduction pathways leading to activation of interferon response factors (IRFs) and NF $\kappa$ B (10, 11). However, one member of the TLR adaptor family, sterile alpha and armadillo motif containing protein 1 (SARM1), is unique in its structure, expression profile, and signaling function. Unlike other TLR adaptor molecules, SARM1 does not activate NF $\kappa$ B or IRF7. Instead, SARM1 has been found to inhibit these signaling pathways following TLR activation of immune cells (12–15). Overexpression of SARM1 or specific domains of SARM1 can lead to cell death, a mechanism recently termed sarmoptosis (12, 16). In the brain, SARM1 is expressed at high levels in neurons and has been linked to neuronal cell death following oxygen glucose deprivation (OGD), viral infection or axonal damage (16–20).

In this current study, we examined the mechanism underlying TLR-mediated neuronal cell death. We found that combined stimulation of TLR7 and TLR9 resulted in neuronal apoptosis in primary cortical neuronal cultures and olfactory sensory neurons, *in vivo*. TLR-induced cell death was not mediated by the normal canonical TLR signaling pathway as MyD88 deficiency had no effect on neuronal apoptosis. Instead, apoptosis was dependent on SARM1 and correlated with SARM1 localization to the mitochondria. Activation of the SARM1 pathway may be an underlying mechanism by which DAMPs, produced during injury or insult to the CNS, contribute to disease pathogenesis by directly stimulating endosomal TLRs and causing neuronal cell death.

## MATERIALS AND METHODS

### Generation of primary cortical neurons and stimulation with TLR ligands

Generation of primary neurons from mice was completed under animal protocol RML2012-56, which was approved by the NIH/NIAID/RML Institutional Animal Care and Use Committee. *Sarm1*<sup>-/-</sup> mice were kindly provided by Michael Diamond, Washington University. These mice as well as *Myd88*<sup>-/-</sup> mice and *Unc93b1* 3D mice (obtained from the Mutant Mouse Regional Resource Center) were maintained on a C57BL/6 background (21). *Tlr7*<sup>-/-</sup> mice were maintained on an Inbred Rocky Mountain White (IRW) background (22). Primary cultures of cortical neurons were prepared from 14 to 16 day gestation mouse

embryos from indicated mouse strains. The cortices were digested in CMF-HBSS containing 0.125% Trypsin followed by dissociation by repeated pipetting. Cells were plated in amine-coated plates (BD Biosciences) at  $8 \times 10^5$  cells/ml. Following attachment, the medium was replaced with maintenance medium composed of neurobasal medium with 2% B-27 and 0.5 mM glutamine.

For TLR stimulation, neuron cultures were treated with optimized concentrations of TLR7 agonist, imiquimod, and TLR9 agonist, CpG-ODN 1826, as determined by a criss-cross assay using serial dilutions of both agonists (data not shown). Concentrations used were 5  $\mu$ M imiquimod and 80 nM CpG-ODN for neurons generated from IRW mice and 5  $\mu$ M imiquimod and 264 nM CpG-ODN for neurons generated from mouse strains with the C57BL/6 background. Strain-specific wildtype controls cultures were generated at the same time as neuron cultures from knockout mice for all experiments. Previous studies with primary neuronal cultures from *Unc93b1* 3D, *TLR7*<sup>-/-</sup> and *MyD88*<sup>-/-</sup> mice demonstrated that these cells are susceptible to LACV-induced apoptosis and thus, are not refractory to cell death (data not shown).

### MTT assay to determine cell viability

Neurons were cultured in 96 well plates and treated with media or agonists using 3–6 replicates per group per experiment. At specific time points, cells were incubated with 3-(4,5-Dimethylthiazol-2-yl)-2,5-Diphenyltetrazolium Bromide (MTT) (Invitrogen) at a concentration of 0.5 mg/ml for 3 hr. The MTT solution was aspirated and DMSO added to each well. The formazan concentration in each well was measured by absorbance at 540 nm using a cell plate reader (Synergy 4, BioTek). Data were compared with mock-infected cultures to determine percent cell death. Cultures from deficient mice were directly compared to WT control cultures generated the same day and treated with the same preparations of TLR agonists.

### Glutamate-induced excitotoxicity in primary neurons

Primary neurons derived from C57BL/6 or *Sarm1*<sup>-/-</sup> mice were treated with two-fold dilutions of kainic Acid (Sigma-Aldrich) or N-Methyl-D-aspartic acid (NMDA, Sigma-Aldrich) to induce cell death. Reagent concentrations and experimental protocol was modeled from Prehn et al., 1994 (23). Briefly, Kainic Acid or NMDA was dissolved in Hank's Buffer Salt Solution (HBSS) containing 5.5 mM D-glucose and added directly to neurons cultured in a 96 well plate for a one hour incubation. Cells were then washed twice with HBSS/glucose before neuronal maintenance media was reapplied and the cells returned to the incubator. After 18hours, cell viability was measured by MTT assay.

### Caspase-3 Detection

Caspase-3 activity was determined using a caspase-3 colorimetric assay kit (GenScript). Cells were incubated in lysis buffer, centrifuged at 10,000 rpm, and the supernatant was collected. Protein content was determined by BCA assay and 300  $\mu$ g of protein with the caspase-3 substrate. The samples were incubated for 6 hr and the extinction values obtained using Synergy 4, Biotek spectrophotometer at 405 nm. Significance was determined by 1-way ANOVA.

### Real-Time PCR

RNA was isolated from primary cortical neurons using Quick-RNA kit (Zymo Research). cDNA was prepared from RNA samples as previously described (24). Primers were designed using primer3 website with a Tm of 60°C (25). SYBR green dye with ROX (Bio-Rad) was used for measurement of real-time PCR amplification. Data for each sample was calculated as the percent difference in CT value ( $CT = CT_{\text{housekeeping}} - CT_{\text{gene of interest}}$ ). The data was plotted as mean average percent of *Gapdh* and beta actin (*Actb*) values for each gene of interest for each sample. Significance was determined by two-way ANOVA. Superarray analysis was completed as previously described (24) using the mouse mitochondrial PCR array (PAMM0087Z). RNA isolated from mock or TLR-stimulated neurons were split evenly between two separate PCR plates for analysis.

### Immunoblot

Mitochondrial fractions from mock and agonist treated primary neurons were isolated using the mitochondria/cytosol fractionation kit (Millipore). Immunoblotting was done using anti-rabbit SARM1 (Genetex GTX77621) as previously described (19). Antibodies to voltage-dependent anion channel 1 (VDAC1) (Abcam ab14734) or cytochrome c oxidase subunit IV (COXIV) Abcam ab14744) were used as a mitochondrial loading controls. Protein was detected using a Typhoon scanner and analyzed with Image Studio Lite software (LI-COR Biosciences).

### Immunocytochemistry analysis of neurons

Primary cortical neurons were grown on poly-D-lysine coated chamber slides. For colocalization studies, cells were fixed and permeabilized at 72 hpi. Cells were co-stained with anti-SARM1 (a gift from Aihao Ding, Cornell University) and heat-shock protein 90 (Abcam, ab13492) or calbindin D (Millipore AB1778) and TUNEL (Promega G7481). Slides were mounted with ProLong Gold antifade reagent with DAPI (Life Technologies). Additional wells were incubated with individual primary antibodies or no primary antibodies prior to incubation with secondary antibodies to confirm the lack of nonspecific staining or cross-reactivity. Digital images were captured using NIS Elements software (Nikon) and compiled using Canvas 14 software (ACD Systems).

### Analysis of cells for mitochondria using mitotracker

Neurons in 8-chambered slides were incubated with 100 nM Mitotracker Red CMX ROS (Life Technologies) and 3.3  $\mu\text{M}$  of Hoechst 33342 dye (Life Technologies) at 37°C for 20–30 minutes. Cells were rinsed one time in PBS and fixed at 37 C for 15 minutes in 3.7% PFA in neurobasal media. Slides were mounted with ProLong Gold antifade reagent (Life Technologies). The slides were analyzed using a Zeiss 510 Meta confocal microscope. For quantification of mitotracker staining, images were analyzed using Zen blue 2011 software. The display of high magnification images were scaled (which did not change the fluorescence values) so that neurite projections could be observed in all images, including mock-stimulated controls. The profile line tool was then used to draw lines down the center of each neurite, with fluorescent intensity measured each 100 nm to control for different lengths of neurites. Individual lines were drawn for branched neurites. Once all lines were

drawn, data tables were generated to show the fluorescent units per 100 nm. Data from multiple images were analyzed for each group and then graphed using Graph-pad Prism to determine differences between groups.

### **Transmission Electron Microscopy analysis of TLR-stimulated cells**

Primary cortical neurons were cultured on Aclar coverslips precoated with poly-D-lysine (0.1 mg/ml) (Sigma). Cells were treated and following 72 hours post stimulation (hps), cells were fixed with 2.5% glutaraldehyde. Samples were prepared for TEM following standard protocols and analyzed using a H7500 microscope (Hitachi high Technologies, Tokyo, Japan). Images were acquired in single-blind experiments.

### **TLR agonist induced cell death of olfactory sensory neurons *in vivo***

OMP-ChR2-YFP (OMP-YFP) knock-in mice, which express enhanced yellow fluorescent protein (YFP) fusion gene from the olfactory marker protein (OMP) locus were purchased from Jackson Laboratories (stock # 014173). YFP is expressed in all olfactory receptor neurons (OSNs) and their nerve terminals of these mice, allowing these neurons to be easily traced (26). Six week old OMP-YFP mice were administered either vehicle control (PBS) or a solution containing a mixture of the TLR agonists imiquimod R837 (25 µg/mouse) and CpG-ODN 1826 (0.5 µg/mouse) intranasally in a volume of 10 µl. Three days after treatment, mice were deeply anesthetized and perfused transcardially with heparin saline (100 U/mL) followed by 10% neutral buffer formalin. Whole skulls were collected and decalcified in 20% EDTA/sucrose for 3 weeks before serially sectioning at 5 µm. Sections were blocked (5% BSA, 0.05% Triton in PBS) at room temperature for 30 min. Primary antibodies against GFP (antibody recognizes YFP protein, 1:500, Ab cam), Caspase 3 (1:250, Promega), SARM1 (1:100, ProSci) or TOM70 (1:150, Sigma-Aldrich) were incubated overnight at 4°C in PBS. Secondary antibodies (donkey anti-goat AF488, donkey anti-rabbit AF594, Invitrogen) were incubated for 1 hr at room temperature. Slides were cover slipped with Prolong Gold antifade mounting media containing DAPI and imaged using a Zeiss 710 LSM (Carl Zeiss) with a Plan Apochromat 63X oil immersion objective (NA 1.40) with a pinhole of 90 µm and a 0.5 µm z-step. Representative images were exported to Imaris v7.7.4 for compilation 4.5 µm maximum intensity projections. All figures were built using Canvas 14 (ACD Systems).

## **RESULTS**

### **TLR7/TLR9 stimulation induces apoptosis of neurons**

Recent studies have found that TLR stimulation of neuronal cultures results in neuronal apoptosis (1, 2, 5–8). We stimulated cultures of primary cortical neurons with the TLR7 agonist, imiquimod, the TLR9 agonist, unmethylated CpG-ODNs, or a combination of both ligands using concentrations of each ligand that were shown previously to be optimal for the activation of both astrocytes and microglia (5). A low level of cell death was observed in neuronal cultures stimulated with either TLR7 or TLR9 ligands, although this level of cell death was variable in replicate cultures and was not generally significant compared to mock-stimulated controls (Fig. 1A, data not shown). In contrast, stimulation of primary cortical

neurons through both TLR7 and TLR9 (TLR7/TLR9) resulted in significantly more cell death compared to mock-stimulated controls or TLR7 or TLR9 stimulation alone (Fig. 1A).

To define the type of neuronal cell death induced by TLR stimulation, we examined cultures for caspase 3 activity, an indicator of apoptotic cell death. Caspase 3 activity was significantly increased in neurons following TLR7/TLR9 stimulation suggesting neuronal apoptosis (Fig. 1B). Immunohistochemical analysis showed an increase in the number of TUNEL-positive nuclei in TLR7/TLR9-stimulated cultures (Fig. 1D) compared to mock-treated cultures (Fig. 1C), also indicating apoptosis. Further confirmation of apoptosis was observed using transmission electron microscopy analysis of TLR-stimulated neurons (Fig. 1E), which showed the classical nuclear condensation associated with apoptosis (27). Thus, stimulation of neurons through TLR7 and TLR9 resulted in neuronal apoptosis.

### TLR-mediated neuronal apoptosis is independent of MyD88 signaling pathway

Since TLR7 agonists have sometimes been found to induce off-target effects independent of the receptor (5), we first confirmed that TLR7/TLR9-induced apoptosis required the presence of TLR7. In TLR7<sup>-/-</sup> neurons, there was a significant decrease in neuronal apoptosis compared to wildtype controls (Fig. 2A), indicating that TLR7 was important for TLR7/TLR9-induced apoptosis. Although TLR7/TLR9 stimulation of TLR7<sup>-/-</sup> neurons still resulted in some apoptosis (Fig. 2A), levels were comparable to those observed with TLR9 agonist stimulation alone (Fig. 1A). Thus, the increased apoptosis observed by the combination of TLR7 and TLR9 ligands together was dependent, in part, on the presence of TLR7.

Both TLR7 and TLR9 signal through the TLR adaptor molecule, MyD88, which leads to the activation of NFκB and IRF7 (11). Cells deficient in MyD88 have inhibited responses to both TLR7 and TLR9 activation (5, 28, 29). We examined whether MyD88 signaling was necessary for TLR7/TLR9-mediated cell death. Surprisingly, neurons from MyD88 deficient mice showed levels of cell death similar to wildtype controls (Fig. 2B), indicating that the canonical pathway for both TLR7 and TLR9 signaling was not necessary for TLR7/TLR9-mediated neuronal apoptosis. Consistent with a lack of MyD88-mediated responses, no detectable upregulation of IL-1α, IL-1β, IL-6 or TNF was observed in neurons following TLR stimulation by multiplex bead analysis (data not shown). Thus, the canonical pathway of TLR signaling through MyD88 to induce cytokine responses was not responsible for TLR-mediated apoptosis.

Since MyD88 was not required for TLR7/TLR9-mediated apoptosis, we next examined whether these receptors were required to be localized to the endosome, which is required for TLR7 and TLR9-mediated cytokine responses (30). We utilized *Unc93b1* 3D mice, which contain a single point mutation in *Unc93b1* that prevents trafficking of TLR7 and TLR9 to the endosome (30). Primary cortical neurons from *Unc93b1* 3D mice were resistant to TLR-mediated apoptosis (Fig. 2B). Thus, TLR-mediated apoptosis was MyD88 independent, but required functional endosomal localization of TLR7 and TLR9.

### **SARM1 localizes to the mitochondria following TLR stimulation of neurons**

Since MyD88 signaling was not required for TLR-induced apoptosis, we looked at other members of the MyD88 family for a potential role in this process. The TLR adaptor molecule SARM1 is a member of this family and is expressed at high levels in neurons (17). SARM1 has also recently been found to mediate Wallerian degeneration as well as contribute to neuronal cell death following bunyavirus infection or OGD (17, 19, 20). Neurons were stained with SARM1 (red fluorescence) and heat shock protein 90 (HSP90) (green fluorescence), which stains both neuronal cell body and neurites. SARM1 (dual yellow fluorescence) localized primarily to the cell body of unstimulated neurons (Fig. 3A), in agreement with recent reports (19, 20). However, TLR stimulation of neurons resulted in increased SARM1 staining in the neurites, as shown by dual staining (white arrows) in these structures (Fig. 3B–C). The increased staining of SARM1 in the neurites was punctate (Fig. 3E), suggesting SARM1 aggregation or localization to an organelle. SARM1 has an N-terminal mitochondrial localization signal and is associated with mitochondria under conditions of neuronal or axonal damage (16, 17, 19, 20). Therefore, we purified mitochondria from neurons and examined them for SARM1. TLR stimulation resulted in increased SARM1 protein in mitochondria fractions (Fig. 3F–G), compared to a modest increase in SARM1 protein levels in the whole cell lysate (Fig. 3H). Thus, TLR stimulation of neurons resulted in increased SARM1 localization to the mitochondria in neurites as determined by both immunocytochemistry and cell fractionation studies.

### **SARM1 is necessary for TLR7/TLR9-mediated neuronal apoptosis**

To determine if SARM1 was necessary for TLR-mediated apoptosis, primary cortical neurons from SARM1 deficient mice were stimulated with TLR agonists. SARM1 deficient neurons did not undergo apoptosis following TLR-stimulation and were comparable to mock-treated controls (Fig. 4A). Thus, SARM1 signaling is a necessary component for neuronal apoptosis following TLR-activation. To confirm that SARM1<sup>-/-</sup> neurons were not just refractory to cell death, we treated primary neuronal cultures with Kainic acid or NMDA to induce cell death (23). Similar cell death curves were observed in wildtype and SARM1<sup>-/-</sup> neurons (Fig. 4B–C). Thus, SARM1 deficiency inhibited TLR7/TLR9-mediated neuronal apoptosis, but not neuronal cell death induced by other mechanisms.

### **TLR-induced SARM1-dependent apoptosis is associated with mitochondrial damage**

As SARM1 localizes to the mitochondria following TLR7/TLR9-stimulation, we stained mitochondrial from mock and TLR7/TLR9-stimulated cells with mitotracker red (Fig. 5A–C). Increased accumulation of mitochondria in neurites was observed in neurons following TLR7/TLR9 stimulation (Fig. 5B) as compared to mock-stimulated neurons (Fig. 5A). Quantification of mitotracker red in neurites showed a significant increase in fluorescence intensity with TLR stimulation (Fig. 5C). Transmission electron microscopy analysis of TLR7/TLR9-stimulated neurons showed accumulation of swollen mitochondria with distorted cristae (Fig. 5E–H) compared to mock-stimulated controls (Fig. 5D,F), indicating that TLR7/TLR9 stimulation induced mitochondrial damage. Analysis of mRNA expression of mitochondria-associated genes demonstrated that TLR7/TLR9 stimulation significantly altered the mRNA expression of several genes associated with apoptosis (*Pmaip1*, *Bcl2l1*,

*Bak1*, *Cdkn2a*, shown in red) as well as inducing a significant down regulation mRNAs for genes involved in small molecule transport (*Slc25a*-associated genes shown in green), outer membrane translocation (*Tomm40*, shown in purple) and mitochondrial fission and fusion (*Cox10* and *Mfn2*, shown in blue) (Fig 6). Thus, TLR7/TLR9-stimulation of neurons results in increased accumulation of damaged mitochondria in neurites as well as altered mRNA expression of mitochondrial associated genes.

### **SARM1 is necessary for mitochondrial accumulation in neurites**

Since SARM1 is required for TLR7/TLR9-induced neuronal apoptosis (Fig. 4A), we examined whether SARM1 deficiency affected the accumulation of mitochondria to neurites. Neurons from SARM1 deficient mice (Fig. 7D) had less extensive localization/accumulation of mitochondria in the neurites compared to wildtype controls (Fig. 7B). Thus, TLR-induced localization/accumulation of mitochondria in neurites was SARM1 dependent. This was consistent with SARM1 localization to the mitochondria (Fig 3D), SARM1 localization to neurites following TLR stimulation (Fig. 3B–C) and TLR-mediated mitochondrial damage in neurons (Fig. 5). Together, these data indicate that TLR activation results in SARM1 localization to the mitochondria and that this localization alters mitochondrial trafficking contributing to SARM1-dependent neuronal apoptosis.

### **TLR7/TLR9-induces neuronal apoptosis in vivo**

The above studies indicate that TLR7/TLR9 can induce apoptosis of neurons, through a SARM1-mediated mechanism that induces accumulation of mitochondria in neurites. To examine if treatment with TLR7/TLR9 stimulation could induce neuronal damage in vivo, we administered agonists intranasally to directly stimulate olfactory sensory neurons (OSNs). Six week old mice expressing enhanced yellow fluorescent protein (YFP) under the olfactory marker protein (OMP) locus were used so that OSNs could easily be identified using anti-GFP antibodies (Fig. 8A). Intranasal administration of TLR7/TLR9 agonists induced neuronal cell death as measured by the loss of OMP-YFP<sup>+</sup> OSNs throughout the olfactory epithelium as well as the reduced intensity of YFP signal in OSN nerve projections (Fig. 8B, D green fluorescence). Active caspase 3 staining was increased in the nasal epithelium of TLR7/TLR9-treated mice (Fig. 8B, red fluorescence) and generally co-localized with YFP<sup>+</sup> OSNs, indicating they were apoptotic (insert). Thus, TLR7/TLR9 stimulation of neurons induces apoptosis in vivo as well as in vitro.

SARM1 expression was observed at low levels in the nasal epithelium, primarily in OSN cell bodies, as well as the mucosal layer of mock-stimulated controls (Fig. 7C red fluorescence, 7E white). However, in TLR7/TLR9 agonist-treated mice, SARM1 was more readily detected in the OSN cell bodies, sensory projections (Fig. 8F, blue arrows) and in the axonal bundles (Fig. 8F, yellow outlines). This indicates that SARM1 expression and localization in OSNs is altered by TLR7/TLR9 stimulation.

Since TLR7/TLR9-mediated neuronal apoptosis was also associated with accumulation of mitochondria in neurites, we also stained for Tom70 to detect mitochondria. Tom70 could be detected at low levels in axon bundles of mock-treated mice and were difficult to detect in the OSN layers (Fig. 9A red fluorescence, 9B–C white arrows). TLR7/TLR9-stimulation



resulted in increased detected of Tom70 in the axon bundles (Fig. 9D red fluorescence, 8E–F white arrows), which appeared more punctate (Fig. 9F white arrows) than in mock-treated controls (Fig. 9C). Additionally, in the OSN layer, intense staining of Tom70 was observed in sensory projections (Fig. 9E, blue arrows), consistent with accumulation of mitochondria in neurites. Thus, *in vivo* TLR7/TLR9 stimulation of OSNs induced similar responses to those observed with cortical neurons *in vitro*, with the induction of apoptosis and the localization/accumulation of SARM1 and mitochondria in neurites and axons. These studies indicate that the TLR7/TLR9 signaling cascade is detrimental to neurons and provides a mechanism of innate-immune mediated neuronal damage in the CNS.

## DISCUSSION

Endosomal TLR activation has previously been shown to induce apoptosis in neurons, although the mechanisms responsible for apoptosis were unknown (1, 5, 6, 8). In the current study, we identified SARM1, a TLR-adaptor molecule, as necessary for TLR7/TLR9-mediated neuronal apoptosis. Thus, neurons appear to have an alternative pathway of activation following endosomal TLR stimulation. This pathway may be specific to neurons, since stimulation of other CNS cells including astrocytes and microglia with the same endosomal TLR ligands results in cytokine production and/or proliferation, rather than cell death (1, 5). SARM1 is expressed at high levels in neurons (17), which may make them more susceptible to TLR-mediated apoptosis.

The mechanism of TLR-induced apoptosis appears to involve mitochondrial trafficking and mitochondrial damage. TLR-induced neuronal apoptosis correlated with SARM1 localization to the mitochondria and increased mitochondrial accumulation in neurites both *in vitro* and *in vivo*. In the absence of SARM1, TLR-induced mitochondrial accumulation in the neurites was inhibited (Fig. 7D). TLR stimulation may alter the normal function of SARM1 in mitochondrial trafficking, resulting in accumulation of normal or damaged mitochondria in neurites. TEM analysis of mitochondria in neurites clearly showed swollen mitochondria with damaged cristae demonstrating that they were not healthy. The increased presence of damaged mitochondria in neurites may lead to increased reactive oxygen species (ROS) generation, as observed in other instances of SARM1-mediated cell death (19), resulting in neuronal apoptosis.

The requirement for UNC93b1 indicates that endosomal localization of TLR7 and TLR9 is essential for mediating neuronal apoptosis. However, the classical MyD88 signaling pathway for both receptors was not essential. This is similar to a previous study, which showed that stimulation of TLR8 induced neuronal apoptosis through a MyD88-independent mechanism (8, 9). The lack of MyD88 involvement in TLR-mediated apoptosis might suggest a direct interaction between endosomal TLRs and SARM1. However, we were unable to co-precipitate SARM1 with either TLR7 or TLR9 in immunoprecipitation assays. This suggests that SARM1 is either not directly interacting with these receptors or that this interaction is weak and unstable. It is also possible those other neuronal proteins provide a link between TLR7/TLR9 and SARM1 activation. Recent studies have shown distinct interactions of TLR7 with non-immune proteins. For example, TLR7 interacts with the cation channel transient receptor potential A1 protein (TRPA1) in pain-sensing neurons,

which affects not only TLR7 function, but also cellular localization (15, 31). Similarly, other neuron-specific proteins could be interacting with TLR7 or TLR9 and triggering the activation of SARM1, leading to neuronal apoptosis.

The MyD88-independent mechanism of neuronal apoptosis observed in this study and in TLR8-induced apoptosis (8, 9) differs from a recent study showing MyD88-dependent neuronal cell death following TLR7 stimulation (1). Thus, endosomal TLR stimulation appears to be able to induce neuronal cell death through both MyD88-dependent and independent mechanisms. We did not observe consistent neuronal cell death with TLR7 stimulation alone using the same ligand as in the above study; however, the concentration of ligand used in our study was approximately 10 fold lower. High concentrations of TLR7 ligand alone may be sufficient to drive MyD88 activation and TNF production resulting in cell death, whereas the combination of lower concentrations of TLR7 and TLR9 ligands may induce a MyD88-independent response resulting in neuronal apoptosis through the activation of SARM1.

Analysis of mRNA expression of mitochondrial associated genes identified multiple genes whose expression was significantly altered following TLR7/TLR9 stimulation. Of these genes, four were associated with regulating apoptosis including *Pmaip1*, *Bak1*, *Bcl2l1* and *Cdkn2a*. *Pmaip1* encodes NOXA, a pro-apoptotic protein that was upregulated, while mRNA for BCL2L1 (BCL-xL), an anti-apoptosis protein, was down regulated. NOXA upregulation and BCL-xL down regulation is associated with oxidative stress induced apoptosis (32) and observed with SARM1-induced apoptosis of neurons following LACV infection (19). Also, down regulation of BCL-xL was associated with SARM1-induced apoptosis in T cells (33), further supporting a link between BCL-2 family members and SARM1-induced apoptosis.

Neuronal death caused by endosomal TLR stimulation in this study was clearly defined as apoptosis as defined by cell morphology, TUNEL staining and caspase 3 activity. This cell death was mediated by SARM1 indicating SARM1 can be involved in the apoptosis pathway. Interestingly, SARM1 was also found to be necessary for Wallerian degeneration in axons, a non-apoptotic process that is not dependent on mitochondrial localization of SARM1 (12, 20). Determining if SARM1 mediates cell death through the same mechanisms for both apoptotic and non-apoptotic cell death will be important in understanding the function of SARM1 in both healthy and damaged neurons.

In the above studies using primary cortical neurons, the combination of TLR7 and TLR9 ligands induced significantly higher levels of neuronal death than either ligand alone. The presence of both TLR7 and TLR9 ligands may occur naturally, not only in the context of a virus or bacterial infection, but also in the case of natural ligands/DAMPs. Recent studies have identified several DAMPs that activate endosomal TLRs including the astrocytic protein stathmin which stimulates TLR3, microRNAs that stimulate TLR7, and DNA from apoptotic cells that activate TLR9 (2–4, 34, 35). The microRNA let-7b was shown to be expressed at high levels in patients with Alzheimer's disease and was released in exosomes from dying neurons and induced neuronal cell death in healthy neurons (2). Another microRNA, miR-21, was found to be elevated in Simian Immunodeficiency Virus (SIV)

encephalitic brains and was neurotoxic (36). As dying neurons would release both microRNAs and cellular DNA, these DAMPs may directly cause death of surrounding neurons by stimulating both TLR7 and TLR9 and induce SARM1 trafficking to the mitochondria. Since microglia in the CNS can also be activated by these same DAMPs and can phagocytose cellular debris, the overall severity of damage to the CNS during neurological disease may be controlled by the balance between the damage to neurons and the ability of microglia to clean up apoptotic and cellular debris that could stimulate cell death in other neurons.

## Acknowledgments

The authors thank Sue Priola, Bruce Chesebro, Leonard Evans, Tyler Moore and Paul Policastro for critical reading of the manuscript. We would also like to thank Mark Albers, Harvard Medical School, with assistance in designing the in vivo model for TLR agonist stimulation.

## Reference List

1. Lehmann SM, Rosenberger K, Kruger C, Habel P, Derkow K, Kaul D, Rybak A, Brandt C, Schott E, Wulczyn FG, Lehnardt S. Extracellularly delivered single-stranded viral RNA causes neurodegeneration dependent on TLR7. *J Immunol.* 2012; 189:1448–1458. [PubMed: 22745379]
2. Lehmann SM, Kruger C, Park B, Derkow K, Rosenberger K, Baumgart J, Trimbuch T, Eom G, Hinz M, Kaul D, Habel P, Kalin R, Franzoni E, Rybak A, Nguyen D, Veh R, Ninnemann O, Peters O, Nitsch R, Heppner FL, Golenbock D, Schott E, Ploegh HL, Wulczyn FG, Lehnardt S. An unconventional role for miRNA: let-7 activates Toll-like receptor 7 and causes neurodegeneration. *Nat Neurosci.* 2012; 15:827–835. [PubMed: 22610069]
3. Fabbri M. TLRs as miRNA receptors. *Cancer Res.* 2012; 72:6333–6337. [PubMed: 23222301]
4. Fabbri M, Paone A, Calore F, Galli R, Gaudio E, Santhanam R, Lovat F, Fadda P, Mao C, Nuovo GJ, Zanesi N, Crawford M, Ozer GH, Wernicke D, Alder H, Caligiuri MA, Nana-Sinkam P, Perrotti D, Croce CM. MicroRNAs bind to Toll-like receptors to induce prometastatic inflammatory response. *Proc Natl Acad Sci U S A.* 2012; 109:E2110–E2116. [PubMed: 22753494]
5. Butchi NB, Du M, Peterson KE. Interactions between TLR7 and TLR9 agonists and receptors regulate innate immune responses by astrocytes and microglia. *Glia.* 2010; 58:650–664. [PubMed: 19998480]
6. Cameron JS, Alexopoulou L, Sloane JA, DiBernardo AB, Ma Y, Kosaras B, Flavell R, Strittmatter SM, Volpe J, Sidman R, Vartanian T. Toll-like receptor 3 is a potent negative regulator of axonal growth in mammals. *J Neurosci.* 2007; 27:13033–13041. [PubMed: 18032677]
7. Liu HY, Chen CY, Hsueh YP. Innate immune responses regulate morphogenesis and degeneration: roles of Toll-like receptors and Sarm1 in neurons. *Neurosci Bull.* 2014; 30:645–654. [PubMed: 24993772]
8. Ma Y, Li J, Chiu I, Wang Y, Sloane JA, Lu J, Kosaras B, Sidman RL, Volpe JJ, Vartanian T. Toll-like receptor 8 functions as a negative regulator of neurite outgrowth and inducer of neuronal apoptosis. *J Cell Biol.* 2006; 175:209–215. [PubMed: 17060494]
9. Ma Y, Haynes RL, Sidman RL, Vartanian T. TLR8: an innate immune receptor in brain, neurons and axons. *Cell Cycle.* 2007; 6:2859–2868. [PubMed: 18000403]
10. Akira S. Toll-like receptor signaling. *J Biol Chem.* 2003; 278:38105–38108. [PubMed: 12893815]
11. Barton GM, Medzhitov R. Toll-like receptor signaling pathways. *Science.* 2003; 300:1524–1525. [PubMed: 12791976]
12. Gerdtz J, Summers DW, Sasaki Y, DiAntonio A, Milbrandt J. Sarm1-mediated axon degeneration requires both SAM and TIR interactions. *J Neurosci.* 2013; 33:13569–13580. [PubMed: 23946415]
13. Siednienko J, Halle A, Nagpal K, Golenbock DT, Miggin SM. TLR3-mediated IFN-beta gene induction is negatively regulated by the TLR adaptor MyD88 adaptor-like. *Eur J Immunol.* 2010; 40:3150–3160. [PubMed: 20957750]

14. Peng J, Yuan Q, Lin B, Panneerselvam P, Wang X, Luan XL, Lim SK, Leung BP, Ho B, Ding JL. SARM inhibits both TRIF- and MyD88-mediated AP-1 activation. *Eur J Immunol.* 2010; 40:1738–1747. [PubMed: 20306472]
15. Yuan S, Wu K, Yang M, Xu L, Huang L, Liu H, Tao X, Huang S, Xu A. Amphioxus SARM involved in neural development may function as a suppressor of TLR signaling. *J Immunol.* 2010; 184:6874–6881. [PubMed: 20483721]
16. Summers DW, DiAntonio A, Milbrandt J. Mitochondrial dysfunction induces sarm1-dependent cell death in sensory neurons. *J Neurosci.* 2014; 34:9338–9350. [PubMed: 25009267]
17. Kim Y, Zhou P, Qian L, Chuang JZ, Lee J, Li C, Iadecola C, Nathan C, Ding A. MyD88-5 links mitochondria, microtubules, and JNK3 in neurons and regulates neuronal survival. *J Exp Med.* 2007; 204:2063–2074. [PubMed: 17724133]
18. Lin CW, Liu HY, Chen CY, Hsueh YP. Neuronally-expressed Sarm1 regulates expression of inflammatory and antiviral cytokines in brains. *Innate Immun.* 2014; 20:161–172. [PubMed: 23751821]
19. Mukherjee P, Woods TA, Moore RA, Peterson KE. Activation of the innate signaling molecule MAVS by bunyavirus infection upregulates the adaptor protein SARM1, leading to neuronal death. *Immunity.* 2013; 38:705–716. [PubMed: 23499490]
20. Osterloh JM, Yang J, Rooney TM, Fox AN, Adalbert R, Powell EH, Sheehan AE, Avery MA, Hackett R, Logan MA, MacDonald JM, Ziegenfuss JS, Milde S, Hou YJ, Nathan C, Ding A, Brown RH Jr, Conforti L, Coleman M, Tessier-Lavigne M, Zuchner S, Freeman MR. dSarm/ Sarm1 is required for activation of an injury-induced axon death pathway. *Science.* 2012; 337:481–484. [PubMed: 22678360]
21. Adachi O, Kawai T, Takeda K, Matsumoto M, Tsutsui H, Sakagami M, Nakanishi K, Akira S. Targeted disruption of the MyD88 gene results in loss of IL-1- and IL-18-mediated function. *Immunity.* 1998; 9:143–150. [PubMed: 9697844]
22. Lewis SD, Butchi NB, Khaleduzzaman M, Morgan TW, Du M, Pourciau S, Baker DG, Akira S, Peterson KE. Toll-like receptor 7 is not necessary for retroviral neuropathogenesis but does contribute to virus-induced neuroinflammation. *J Neurovirol.* 2008; 14:492–502. [PubMed: 19016073]
23. Prehn JH V, Bindokas P, Marcuccilli CJ, Krajewski S, Reed JC, Miller RJ. Regulation of neuronal Bcl2 protein expression and calcium homeostasis by transforming growth factor type beta confers wide-ranging protection on rat hippocampal neurons. *Proc Natl Acad Sci U S A.* 1994; 91:12599–12603. [PubMed: 7809085]
24. Du M, Butchi NB, Woods T, Morgan TW, Peterson KE. Neuropeptide Y has a protective role during murine retrovirus-induced neurological disease. *J Virol.* 2010; 84:11076–11088. [PubMed: 20702619]
25. Untergasser A, Cutcutache I, Koressaar T, Ye J, Faircloth BC, Remm M, Rozen SG. Primer3--new capabilities and interfaces. *Nucleic Acids Res.* 2012; 40:e115. [PubMed: 22730293]
26. Smear M, Shusterman R, O'Connor R, Bozza T, Rinberg D. Perception of sniff phase in mouse olfaction. *Nature.* 2011; 479:397–400. [PubMed: 21993623]
27. Ziegler U, Groscurth P. Morphological features of cell death. *News Physiol Sci.* 2004; 19:124–128. [PubMed: 15143207]
28. Heil F, Ahmad-Nejad P, Hemmi H, Hochrein H, Ampenberger F, Gellert T, Dietrich H, Lipford G, Takeda K, Akira S, Wagner H, Bauer S. The Toll-like receptor 7 (TLR7)-specific stimulus loxoribine uncovers a strong relationship within the TLR7, 8 and 9 subfamily. *Eur J Immunol.* 2003; 33:2987–2997. [PubMed: 14579267]
29. Hemmi H, Kaisho T, Takeuchi O, Sato S, Sanjo H, Hoshino K, Horiuchi T, Tomizawa H, Takeda K, Akira S. Small anti-viral compounds activate immune cells via the TLR7 MyD88-dependent signaling pathway. *Nat Immunol.* 2002; 3:196–200. [PubMed: 11812998]
30. Tabeta K, Hoebe K, Janssen EM, Du X, Georgel P, Crozat K, Mudd S, Mann N, Sovath S, Goode J, Shamel L, Herskovits AA, Portnoy DA, Cooke M, Tarantino LM, Wiltshire T, Steinberg BE, Grinstein S, Beutler B. The Unc93b1 mutation 3d disrupts exogenous antigen presentation and signaling via Toll-like receptors 3, 7 and 9. *Nat Immunol.* 2006; 7:156–164. [PubMed: 16415873]

31. Winkler CW, Taylor KG, Peterson KE. Location is everything: let-7b microRNA and TLR7 signaling results in a painful TRP. *Sci Signal*. 2014; 7:e14.
32. Eno CO, Zhao G, Olberding KE, Li C. The Bcl-2 proteins Noxa and Bcl-xL co-ordinately regulate oxidative stress-induced apoptosis. *Biochem J*. 2012; 444:69–78. [PubMed: 22380599]
33. Panneerselvam P, Singh LP, Selvarajan V, Chng WJ, Ng SB, Tan NS, Ho B, Chen J, Ding JL. T-cell death following immune activation is mediated by mitochondria-localized SARM. *Cell Death Differ*. 2013; 20:478–489. [PubMed: 23175186]
34. Bsibsi M, Bajramovic JJ, Vogt MH, van DE, Baghat A, Persoon-Deen C, Tielen F, Verbeek R, Huitinga I, Ryffel B, Kros A, Gerritsen WH, Amor S, van Noort JM. The microtubule regulator stathmin is an endogenous protein agonist for TLR3. *J Immunol*. 2010; 184:6929–6937. [PubMed: 20483774]
35. Hsiao HB, Chou AH, Lin SI, Chen IH, Lien SP, Liu CC, Chong P, Liu SJ. Toll-like receptor 9-mediated protection of enterovirus 71 infection in mice is due to the release of danger-associated molecular patterns. *J Virol*. 2014
36. Yelamanchili SV, Lamberty BG, Rennard DA, Morse BM, Hochfelder CG, Meays BM, Levy E, Fox HS. MiR-21 in Extracellular Vesicles Leads to Neurotoxicity via TLR7 Signaling in SIV Neurological Disease. *PLoS Pathog*. 2015; 11:e1005032. [PubMed: 26154133]

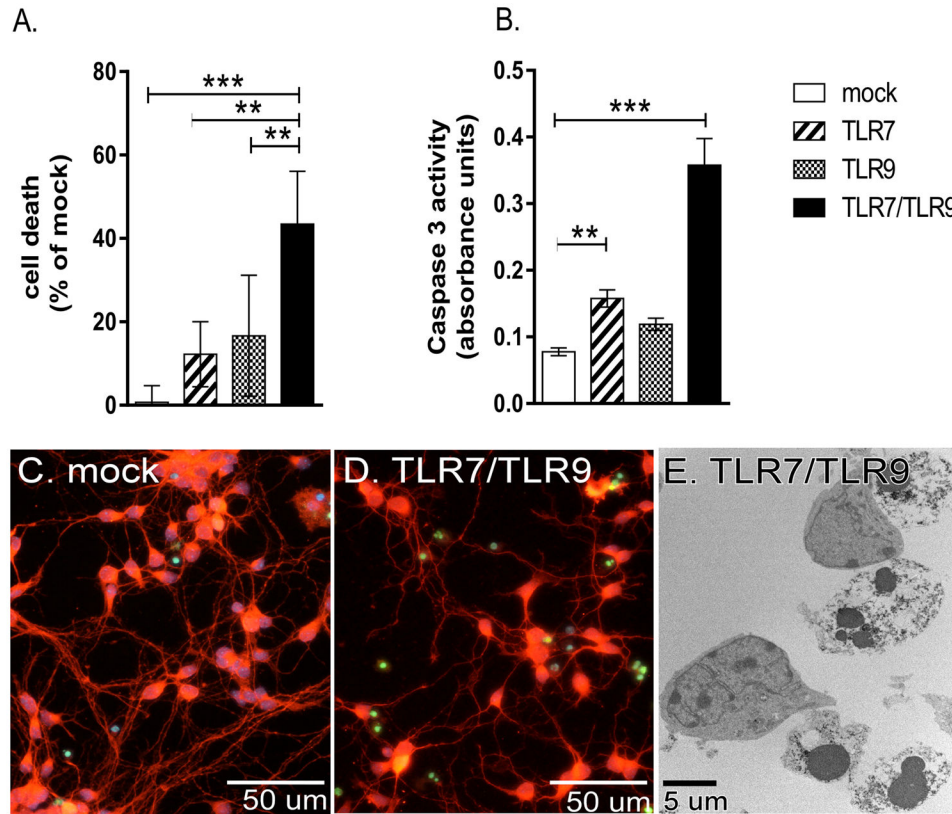


**Figure 1. Combined TLR7 and TLR9 stimulation results in significant neuronal apoptosis** (A–D) Primary cortical neurons were stimulated with either the TLR7 ligand (imiquimod), TLR9 ligand (CpG-ODN) or both agonists for 72 hours and then analyzed for cell death by (A) MTT assay or (B) Caspase 3 activity. Data are the mean  $\pm$  standard deviation (SD) of 4 to 6 samples per group and are representative of 2 to 3 replicate experiments. Significance was determined by One-way ANOVA with Bonferroni's multiple comparison post-test. \*\*  $P < 0.01$ , \*\*\*  $P < 0.001$ . (C–D) Representative images from (C) mock and (D) TLR7/TLR9 stimulated neurons stained with Calbindin D (red fluorescence) to detect neuronal bodies and TUNEL (green fluorescence) to detect apoptotic cells. (E) TLR7/TLR9-stimulated neurons underwent apoptosis showing nuclear condensation and blebs by TEM.

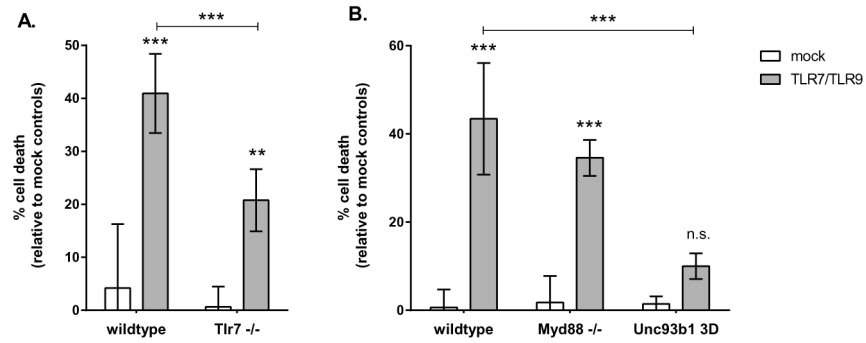


**Figure 2. TLR7/TLR9-induced apoptosis requires endosomal localization but is not mediated by MyD88 signaling**

(A) Primary cortical neurons were generated from wildtype (IRW) or *Tlr7*<sup>-/-</sup> mice and stimulated with a combination of TLR7 and TLR9 ligands as described in Fig. 1. Cell death was measured at 72 hps by MTT assay. (B) Neurons from wildtype (C57BL/6), *Myd88*<sup>-/-</sup> or *Unc93b1* 3D mice were stimulated with a combination of TLR7 and TLR9 ligands and measured for cell death at 72 hps by MTT assay. Data are the mean  $\pm$  SD of 4 to 6 samples per group and are representative of 2 to 3 replicate experiments. Statistical analysis was completed by two-way ANOVA with Dunnett's multiple comparison test. \*\* P<0.01 \*\*\* P<0.001. n.s. = not significant.

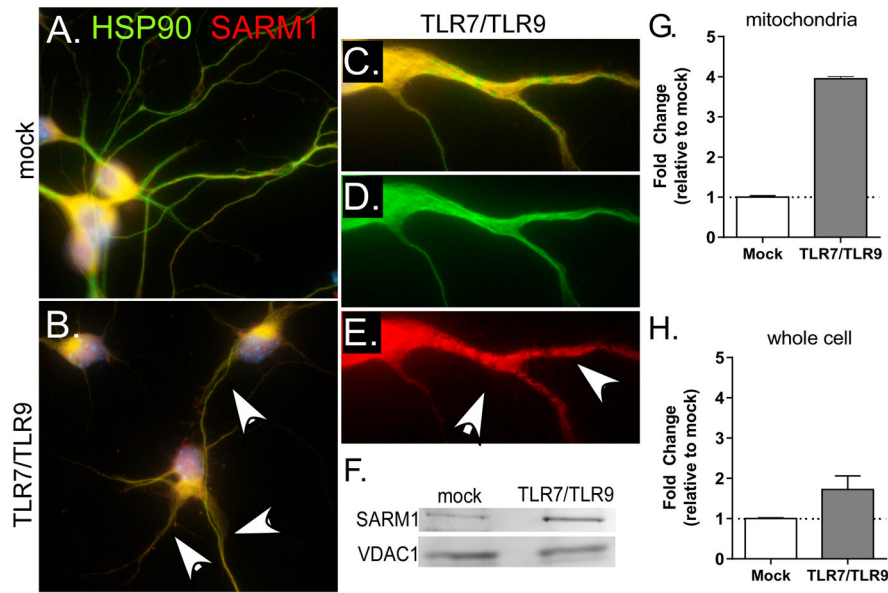


### Figure 3. SARM1 localizes to neurites following TLR7/TLR9 stimulation

Primary cortical neurons were stimulated with TLR7 and TLR9 ligands or mock controls. (A–E) Cells stained with HSP90 (green fluorescence) to identify neuronal cell delimitations and SARM1 (red fluorescence). SARM1 was observed primarily in the cell bodies (yellow dual fluorescence), but not the neurites of (A) mock-infected cells. However, (B–E) TLR stimulated neurons generally showed retracted neurites with focal areas of increased SARM1 (white arrows). (C–E) Close up showing punctate staining of SARM1 in neurites with (C) dual staining, (D) HSP90 and (E) SARM1. Images are representative of 2–3 repeated experiments. (F) Mitochondria were isolated from neurons at 72 hps and examined for the amount of SARM1 protein by western blot. VDAC1 was used as a loading control. (G–H) Quantification of SARM1 protein in (G) mitochondrial fraction normalized to VDAC1 expression as well as (H) whole cell lysates normalized to  $\beta$ -actin expression. Data are shown as fold change relative to mock controls. Error bars represent the range of 2 samples per group.



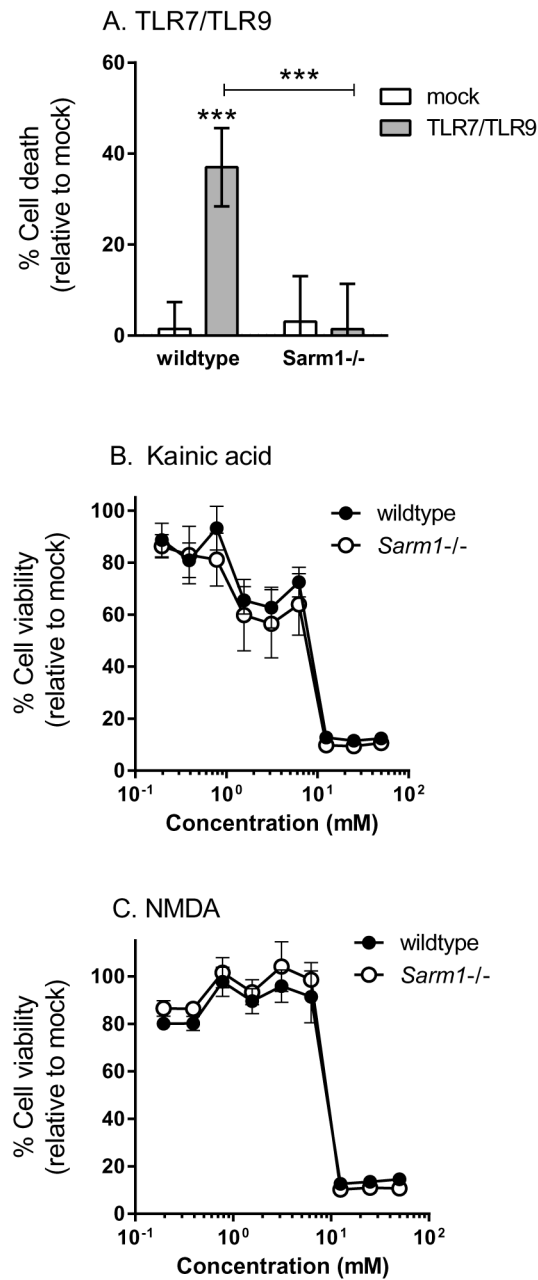


**Figure 4. SARM1 is required for TLR7/TLR9-mediated neuronal apoptosis**

(A–C) Primary cortical neurons from wildtype (C57BL/6) or *Sarm1*<sup>-/-</sup> mice were stimulated with (A) TLR7/TLR9 agonists (B) Kainic acid or (C) NMDA and analyzed for cell death at (A) 72 hps or (B–C) 18 hps. (A) Wildtype, but not SARM1<sup>-/-</sup> neurons underwent apoptosis following TLR7/TLR9 stimulation. Data are the mean ± SD for 4–12 samples per group and are representative of 2–3 replicate experiments. (B–C) Wildtype and SARM1<sup>-/-</sup> neurons were treated with two-fold dilutions of (B) kainic acid or (C) NMDA. No statistical difference was observed between wildtype and SARM1<sup>-/-</sup> neurons for either drug. Data are the mean ± SD for 6 samples per group per concentration. Statistical analysis

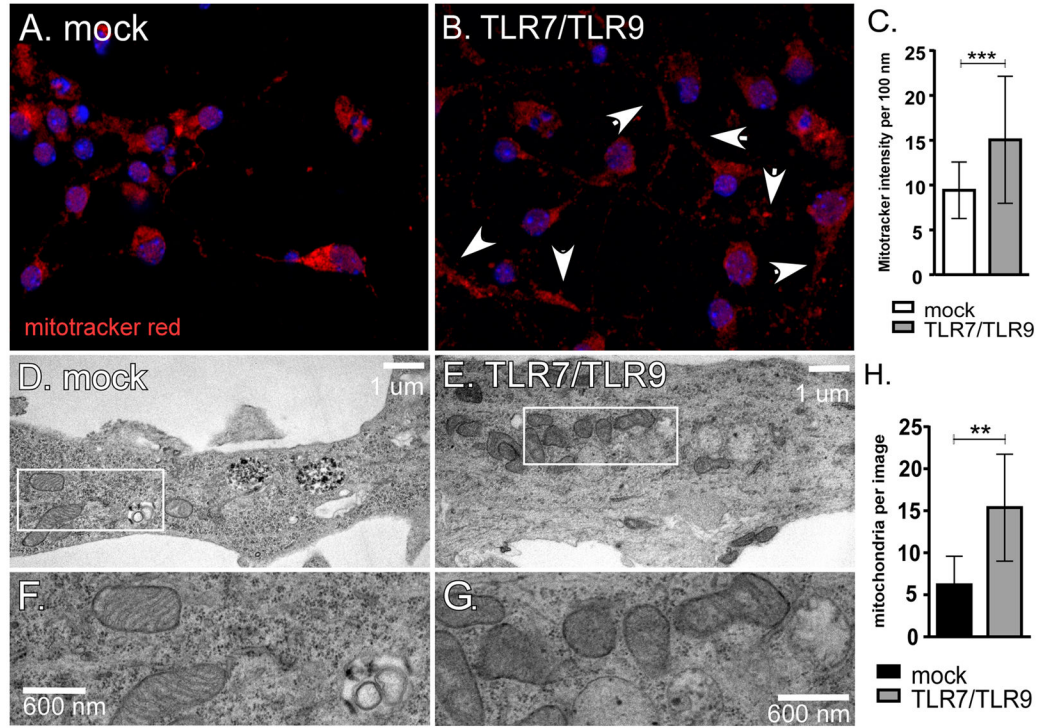
was completed with a two-way ANOVA with a Bonferroni's multiple comparison post-test.  
\*\*\* P<0.001.

Author Manuscript

Author Manuscript

Author Manuscript

Author Manuscript

**Fig. 5.**

TLR7/TLR9 stimulation induces mitochondrial damage in neurons.

(A–C) Neurons were stained for mitochondria using MitoTracker Red CMXRos dye (red fluorescence). (B) Increased mitochondria in the neurites were observed (white arrows) following TLR7/TLR9 stimulation. (C) Mitotracker intensity in neurites was measured as fluorescence per 100 nm for multiple neurites in mock or TLR7/TLR9-stimulated cultures using Zen 2011 software. Data are the mean  $\pm$  SD of 200–244 data points per group. Statistical analysis was completed using Mann Whitney test. \*\*\*  $P < 0.0001$  (D–H) Primary cortical neurons grown on Aclar coverslips were mock-stimulated or stimulated with TLR7/TLR9 ligands for 72 hrs. Cells were fixed and prepared for TEM. (D) TEM of mock-infected culture showing healthy mitochondria in a neurite. (E) TEM image of TLR7/TLR9-stimulated culture showing swollen neurite containing over 20 mitochondria in the field of view. (F–G) Enlarged image of mitochondria from box in (D) and (E) showing (F) healthy mitochondria and (G) mitochondria with distorted cristae. Images are representative of cells for both groups. Scale bars are shown for each sample. (H) Number of mitochondria in neurites per image. Images of the same magnification from mock-stimulated cultures and TLR7/TLR9-stimulated cultures were analyzed for the number of mitochondria in the neurites. Data are the mean  $\pm$  SD from 10 mock images and 8 TLR7/TLR9 images. Statistical analysis was completed using Mann Whitney test. \*\*  $P < 0.01$

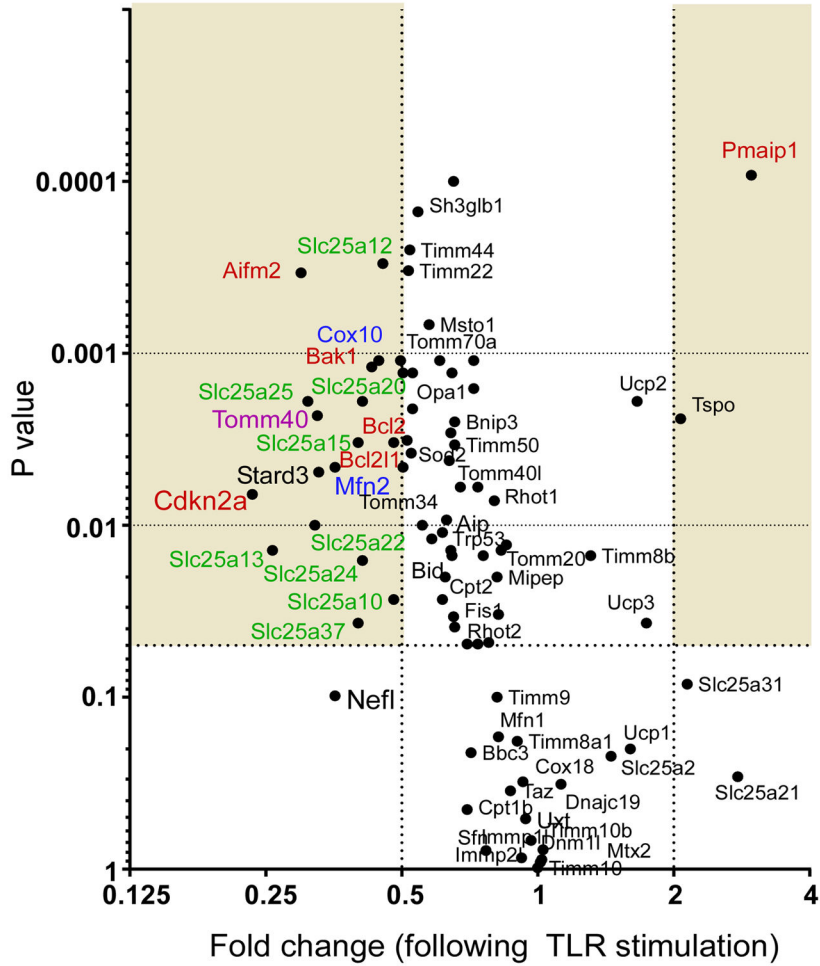


**Figure 6. TLR7/TLR9-stimulated neurons have altered mRNA expression of mitochondrial related genes**  
 PCR-array analysis of 84 genes involved in biogenesis and function of the mitochondria. RNA was isolated from four mock and four TLR7/TLR9-stimulated neuron samples at 72 hps from two separate experiments and analyzed by real-time PCR array. Data are plotted as fold change between mock and TLR-stimulated samples (X axis) versus P value (Y axis). Shaded areas indicate at least a two-fold difference with a P value less than 0.05.

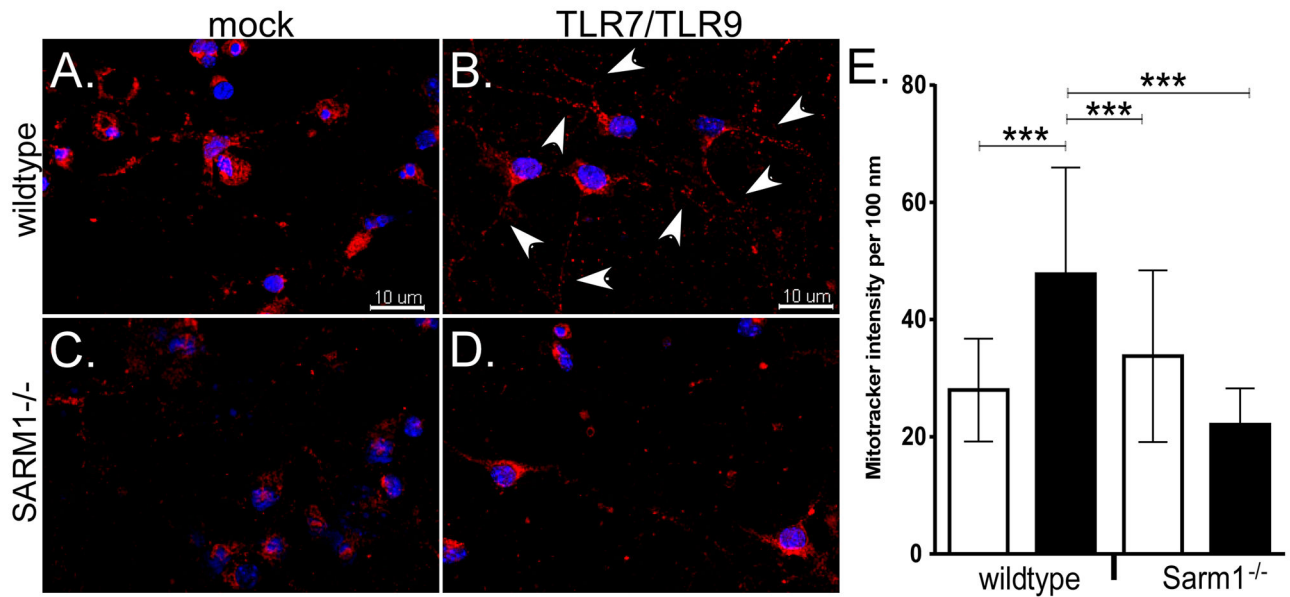


**Figure 7. SARM1 deficiency results in decreased mitochondrial accumulation in neurites**  
 Primary cortical neurons from (A–B) wildtype or (C–D) *Sarm1*<sup>-/-</sup> mice were stimulated with (B,D) TLR7/TLR9 ligands or (A,C) mock-stimulated. At 60 hps, neurons were incubated with MitoTracker Red CMXRos dye (red fluorescence) to detect mitochondria and Hoechst 33342 dye (blue fluorescence) as a counterstain. (B) white arrows show increased mitochondria (red fluorescence) in the neurites of neurons in TLR7/TLR9 stimulated cultures compared to (A) mock-treated cultures. (D) This increase of mitochondria in neurites was not observed in TLR7/TLR9-stimulated *Sarm1*<sup>-/-</sup> neurons. Images are representative of cultures for each group. (E) Quantification of mitotracker intensity in neurites. Red fluorescence intensity per every 100 nm was measured in neurites from mock and TLR7/TLR9-stimulated wildtype and *SARM1*<sup>-/-</sup> neurons. Data are the mean ± SD for 76–187 individual data points per group and include measurements from multiple neurites per image and multiple images per group. Statistical analysis was completed using One-way ANOVA with a Tukey’s multiple comparison test between all groups. \*\*\* P<0.0001

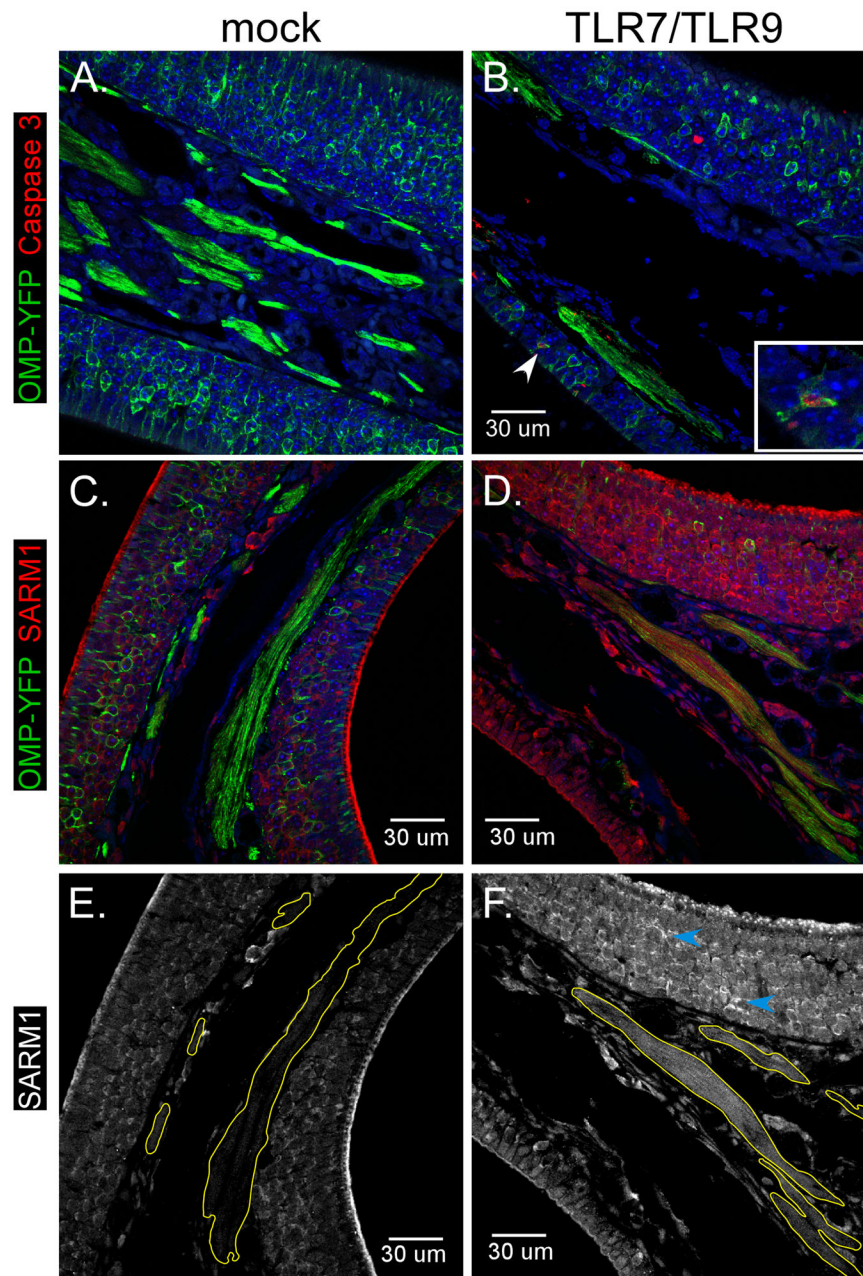


**Figure 8. TLR7/TLR9 stimulation induces neuronal apoptosis and SARM1 upregulation in OSNs**

Six week old OMP-YFP mice were administered intranasally (A,C, E) PBS or (B,D, E) PBS containing 25  $\mu$ g of imiquimod and 0.5  $\mu$ g of CpG-ODN 1826. At 72 hps, tissues were removed and processed for immunohistochemistry. (A–F) Nasal epithelium from (A, C, E) mock or (B, D, F) TLR agonist-inoculated mice were stained with (A–D) anti-GFP to detect OSNs (green fluorescence) and either (A–B) anti-active caspase 3 or (C–F) SARM1. Inset in (B) shows OMP-YFP positive OSN that is also positive for Caspase 3. (E–F) Only fluorescence of SARM1 is shown which demonstrates increase in SARM1 staining in OSN

layer and axonal bundles (yellow outline) of TLR-stimulated mice. Blue arrows indicate SARM1 staining of OSN projections. All error bars are 30  $\mu$ m.

Author Manuscript

Author Manuscript

Author Manuscript

Author Manuscript

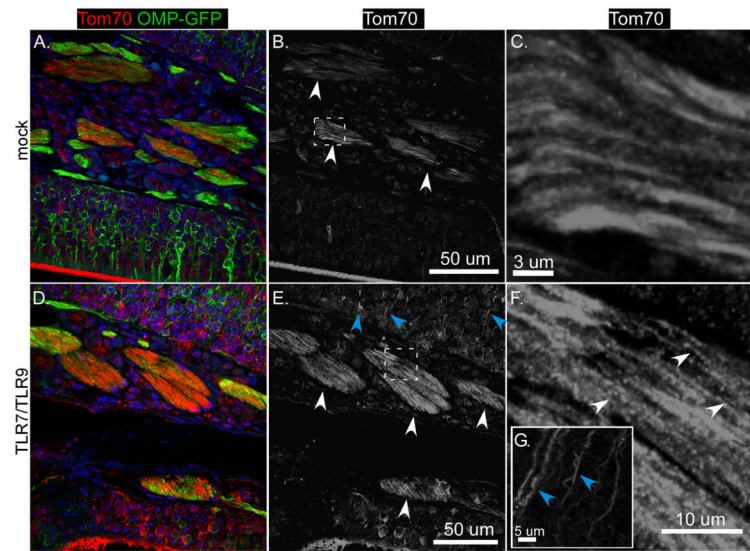


**Figure 9. TLR7/TLR9 stimulation alters mitochondrial localization in nasal epithelium**  
 Tissue sections from mice identified in Fig. 8 were also analyzed for mitochondria localization using an anti-Tom70 antibody (red fluorescence). Sections from (A–C) Mock or (D–F) TLR agonist-inoculated mice show differences in Tom70 staining (red fluorescence, primarily in the axonal bundles (Fig. B, E, white arrows). (C, F) Higher power images of these bundles show more punctate staining (white arrows) in (F) TLR-treated mice compared to (C) mock-treated mice. (E) Blue arrows indicate Tom70 staining of OSN projections in TLR-treated mice.